

Overview of Optical Techniques That Measure Displacements: Murray Lecture

by Cesar A. Sciammarella

ABSTRACT—Optical techniques that measure displacements play a very important role in current experimental mechanics, material sciences and metrology. This paper presents a survey of developments in these techniques from a personal experience point of view. Three main aspects are considered. Mathematical and numerical models used in the interpretation of fringe information and the corresponding data processing techniques. Optical and electro-optical developments that have taken place to improve the sensitivity, and the efficiency of these methods to make them competitive with purely numerical methods. Applications that have arisen from the synergy between advanced computational capabilities and optics are also presented.

KEY WORDS—Optical techniques to measure displacements, moiré, holography, moiré-holography, holographic-moiré, speckle interferometry, electro-optic holography, Fourier analysis of fringe patterns.

Introduction

Optical Techniques that Measure Displacements and Contouring Techniques

Several optical techniques can be used to measure displacements on the surfaces of solid bodies. Typically, these techniques have been developed separately, although occasionally connections between them have been pointed out. In chronological order, moiré was the first technique to be developed, which was followed by holography, speckle photography, speckle interferometry and numerical correlation of speckles, either formed by using coherent illumination or by applying random patterns to a surface.

The purpose of using any of these techniques is to find displacement fields on surfaces, either external on opaque media or internal in transparent media.

Concurrently with the measurement of displacements, optical techniques have been used to obtain contours of surfaces in the case of light diffusing surfaces, and slopes on reflecting surfaces. All the different techniques mentioned here can be used for these two purposes. Metrological applications involving contouring is the one area that has experienced the largest industrial development.

Cesar A. Sciammarella (SEM Member) is a Professor, Mechanical Materials and Aerospace Engineering, Illinois Institute of Technology, Chicago, IL 60611.

Original manuscript submitted: February 24, 2002.
Final manuscript received: July 13, 2002.

Measurement of Displacement or Contour Information by Optical Techniques

The first step in the process of generating displacement or contour data is to have a carrier on the surface under observation. A carrier is a known signal that will be modified upon changes of the surface. There are three ways to obtain this information. The carrier can be intrinsic to the surface; in this case, both displacement and contour information can be obtained. The carrier can be projected onto the surface; in this case, displacement or coordinates with respect to a reference plane can be obtained. If the surface is a reflective surface, the slope of the surface is obtained. The carrier can be a deterministic signal, a so-called Ronchi grating, or it can be a random pattern from which optically or numerically coordinates or displacements can be obtained. Similar statements can be made with respect to the measurement of slopes by using reflecting surfaces.

There are two ways that we can extract the information from a carrier. If the optical system can detect the carrier, the change of geometry or modulation of the carrier directly provides the sought information. If the carrier cannot be observed because it is beyond the optical resolution of the observation system, the moiré effect can be used. The moiré effect is the beat signal of the deformed carrier with the undeformed carrier used as a reference or master. The beat signal can be produced by using coherent light, taking advantage of the phenomenon of interference (moiré interferometry, holographic interferometry, speckle interferometry). In addition, incoherent light methods can be used and the beat fringes can be produced by superposition of intensities (moiré, speckle photography, numerical correlation methods). In the case of moiré, speckle photography, and numerical correlation if we use the double exposure method, i.e., if we take the initial and final images on the same exposure, the optical system must be able to resolve the carrier. This circumstance puts a limit on the frequency of the carrier that can be used and therefore on the spatial frequencies that can be recovered.

Analytical and Numerical Models for Fringe Pattern Analysis

Relationship between Methods that Provide Displacements and Continuum Mechanics

In 1957, Dantu¹ introduced the basic theory that connects moiré fringe patterns with continuum mechanics. He defined the moiré fringes as loci of the points of a surface that have the same projected displacement in the direction

perpendicular to the carrier direction. If we take x -coordinates in the horizontal direction and y -coordinates in the vertical direction, the displacements in the x -direction or $u(x, y)$ displacements are obtained from vertical carriers, and the vertical displacements $v(x, y)$ are obtained from horizontal carriers. The moiré fringes were called isotetic lines by Durelli and Parks² (lines of equal displacement). The original derivations of Dantu were limited to small-deformation and small-rotation continuum mechanics. In 1960, Sciammarella³ generalized the theory to large deformations, showing that moiré fringes provide the displacement information in the geometry of the deformed body, Eulerian description in continuum mechanics, and that moiré fringe information can be used to generate any desired form of the strain tensor. Geometrical properties of the moiré fringes analyzed as level lines of the Monge representation of the projected displacement surfaces $u(x, y)$, $v(x, y)$ and their gradients have been studied. Families of lines associated with the isotetic lines, lines with zero projected displacement and lines with zero rotation have been defined as well as singular lines (lines with zero displacement and zero rotation) and singular points. Complete sign conventions have been introduced. Although derived in the context of moiré fringes, these properties are properties of the isotetic lines and therefore apply to any of the techniques that provide displacement information.

Generalization of the Concept of Fringe Order

The concept of fractional fringe order is familiar to photoelasticians. In 1929 Tardy⁴ provided an optical procedure to measure fractional fringe orders. The fringe order concept relates in photoelasticity the light intensity of a given point of a field to the relative retardation at the same point. No such concept existed in moiré fringes. In the original literature of moiré fringes, points of minima have been assumed as data points and the projected displacement curves have been plotted as staircase plots.⁵ In the fall meeting of SESA of 1964, Sciammarella⁶ presented the displacement light-intensity moiré optical law. The law was derived using the Fourier analysis of the formation of images with incoherent light. It was shown that, if the first harmonic of the fringe pattern was obtained, the moiré signal could be represented by

$$I(x) = I_o + I_1 \cos 2\pi\rho(x). \quad (1)$$

In eq (1), I_o is the background intensity, and I_1 is the first harmonic of the image intensity. The quantity $\rho(x) = n(x)$ is the generalization of the fringe order concept; n is no longer an integer. The importance of eq (1) is that it provides a continuous relationship between light intensity at a given point and its displacement. From the property of moiré fringes, the argument of eq (1) gives the projected displacement,

$$u(x) = \left[\frac{1}{2\pi} \arccos \frac{I(x) - I_o}{I_1} \right] p, \quad (2)$$

where p is the pitch of the grating. Quoting Sciammarella:⁶ "Fractions of the grid pitch can be measured and in order to increase sensitivity it is no longer necessary to increase the number of grid lines." The validity of this statement has been supported by all the experience accumulated in the application of moiré and other techniques that measure displacements. The obvious question is how far can we go in measuring fractions of a pitch. As we are going to see, it

took a long time before a satisfactory answer to this question could be obtained. Sciammarella⁶ has stated that, although the moiré optical law was derived for incoherent illumination, eq (1) was a general tool for dealing with all moiré phenomena irrespective of the mechanism of formation of the fringes. Practical applications were illustrated in the second part of the paper,⁷ where a device to measure light intensities was presented. This work resulted in a US patent of a device for highly accurate digitalization of photographic recording of fringes.

Application of the Moiré Optical Law to Computer-aided Fringe Analysis

The first attempts to use the continuous law in practical applications demonstrated that the fringe profiles obtained from the photo-scanning device had several sources of noise, which it was necessary to remove. Moiré fringes in a tensile specimen were analyzed.⁸ The fringes revealed several sources of noise, changes of the background intensity I_o , changes of amplitude of the first harmonic I_1 , local noise and distortions of fringe profiles. Corrections were introduced, an error analysis was carried out and it was shown that displacements to $p/70$ could be accurately measured. Sciammarella and Sturgeon⁹ have presented substantial improvements in the processing of moiré data. Band-pass digital filters were applied to separate background intensity from the first harmonic. At the same time, band-pass filters in quadrature were introduced to separate the amplitude modulation of the first harmonic from the phase modulation. A process of numerical differentiation was introduced to obtain strains from displacements. A disk under diametrical compression was used as an example of application. In the same paper, the Fourier transform properties of lenses in coherent and incoherent illumination were applied to optically filter moiré patterns with coherent and incoherent illumination. In the same year, in the fall meeting of SESA,¹⁰ a more detailed presentation of the concept of moiré fringes as frequency-modulated signals was introduced. At the same time, the subject of digital filters to separate the first harmonic and remove noise and the concept of filters in quadrature were discussed more extensively.

The model of fringe formation introduced by Sciammarella and Sturgeon¹⁰ is shown in Fig. 1. This model has been quite successful in handling other aspects of fringe pattern analysis. This model is applicable to moiré fringes or to the carrier signal. In Fig. 1, the model is applied to a carrier. The carrier is a sinusoidal function generated by a rotating vector \mathbf{E} and the phase of a point of coordinate x is defined as the total angle rotated by the vector up to that point. The modulation function $\Psi(x)$ is the projected displacement function transformed into an angular variable. The total phase of the carrier is the addition of the phase generated by the constant rotation plus the modulation function contribution. Without loss of generality and referring to the component of the displacement projected in the x -direction, the modulation function is

$$u(x) = \frac{p\Psi(x)}{2\pi}. \quad (3)$$

The quantity $\rho(x)$ is given by

$$\rho(x) = \frac{\Psi(x)}{2\pi}. \quad (4)$$

The instantaneous angular velocity of the vector is

$$\varepsilon(x) = \frac{p}{2\pi} \frac{\partial \Psi(x)}{\partial x}. \quad (5)$$

The displacement field of a surface is represented by two modulation functions $\Psi_x(x, y)$ and $\Psi_y(x, y)$ that can be obtained from two orthogonal system of grids. The projected displacement functions are not provided directly but they are encoded in sinusoidal signals. If we substitute eq (3) into eq (1), we obtain the expression of the moiré fringes originated by the superposition of the deformed and undeformed carriers. In the same way that the equation for moiré fringes is derived, we can derive for the deformed carrier the equation

$$I(x) = I_{oc} + I_{1c} \cos(2\pi f_c x + \Psi(x)), \quad (6)$$

where $f_c = 1/p$ is the carrier frequency. We can see that if the carrier is recorded, the modulation function can be obtained directly from the carrier without forming the moiré fringes. Figure 2 illustrates the concept of digital filtering in the Fourier transform (FT) space. The filter recovers the first harmonic of the signal spectrum and removes the noise composed of higher harmonics and other components. Figure 3 illustrates the in-phase component and the in-quadrature component; the phase of the rotating vector can be obtained by the equation

$$\Psi(x) = \arctg \frac{I_q}{I_p}. \quad (7)$$

By knowing the in-phase component, it is possible to find the in-quadrature component since they are related through the Hilbert transform. Sciammarella and Sturgeon¹⁰ have applied the process of fringe pattern analysis to a tensile specimen, and the error analysis indicated that displacements were accurately measured to $p/360$. To apply the moiré optical law, it is necessary to measure relative light intensities. The measurement has to be made through some recording medium that, in general, will introduce distortions on the signal. In the fall meeting of the Society for Experimental Mechanics (SEM) in 1967,¹¹ the effect of the non-linearity of the recording medium was addressed. It was shown that the effect of the non-linearity was to generate harmonics of the fundamental signal. It was proven that the fundamental harmonic could be recovered even in the case of strong saturation of the signal that results in the flattening of its maximum. Large amplitude modulations caused by non-uniformity of the illumination also were taken into account by the filters in quadrature.

Through the described developments, the moiré optical law was established on a solid theoretical and practical foundation. As a result, computer-aided fringe pattern analysis became a reality.

Further Developments of the Fourier Analysis of Fringe Patterns

In 1966,⁹ the analysis of strains along the diameter of a compressed disk was presented as an example of the use of digital filters in quadrature. At the time, the problem of fringe phase unwrapping was not solved and, since phases were given to modulus π , differentiation was performed pointwise on the wrapped phase. The same problem was again tackled in a more complete form and the results were presented in the meeting of SEM in 1968. In this presentation, the full process

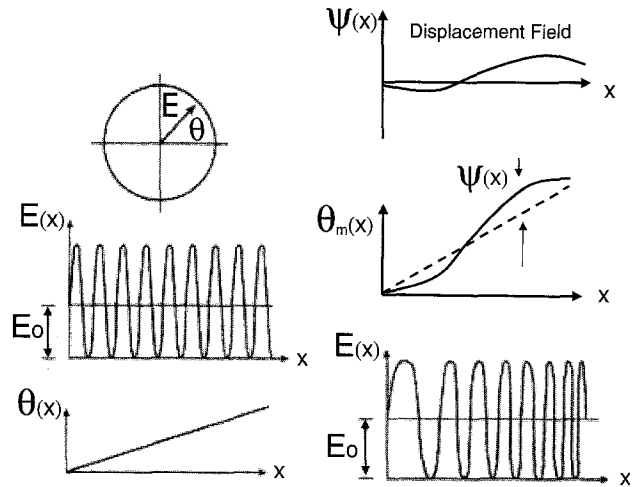


Fig. 1—Graphical representation of the process of modulation of a carrier

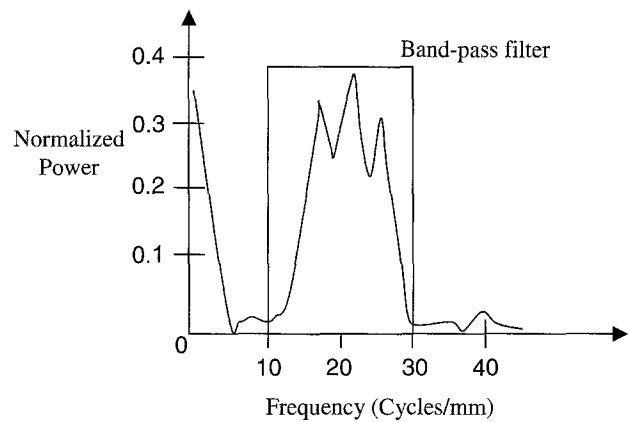


Fig. 2—The band-pass filter removes background intensity and noise, and passes the components of the first harmonic of the space-modulated fringe pattern

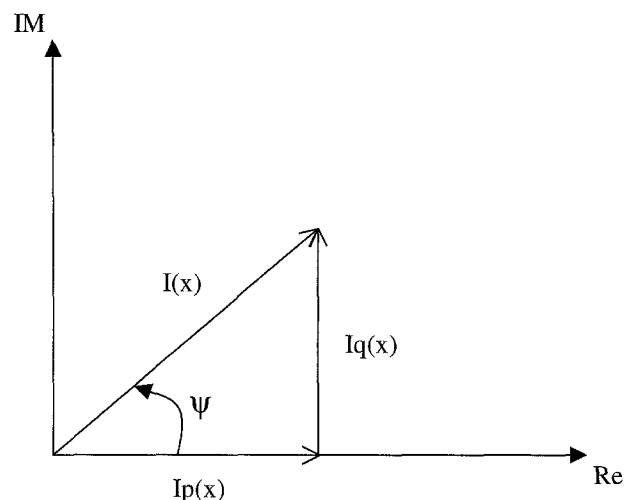


Fig. 3—Vectorial representation of the in-quadrature signals

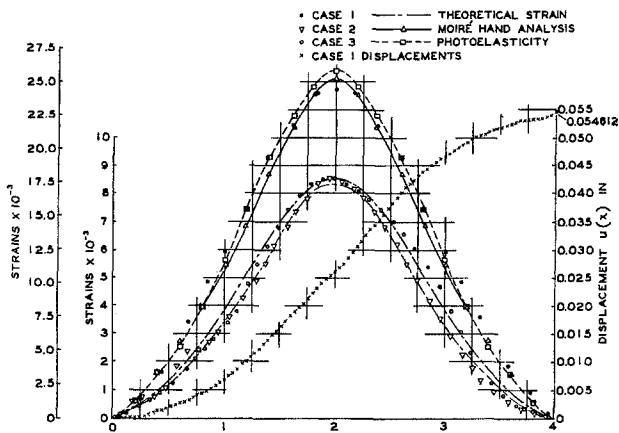


Fig. 4—Displacements and strains obtained by computer processing patterns of a disk under diametrical compression (1968)

of the Fourier method of fringe analysis was introduced. Figure 4, taken from the written version of the material presented in 1968¹² shows the unwrapped phase and the strains for three fringe patterns. One of the fringe patterns was a regular moiré fringe pattern; the other two included an initial or reference pattern (carrier fringes) generated by using reference gratings of different pitches from the grating printed in the model. Figure 5 shows the FT power spectrum of the analyzed patterns. A flow chart was given of the FORTRAN computer program utilized in this study. The process included the extension of the signals beyond the boundaries to take care of edge effects caused by the fact that, in view of the filter symmetry at the end-points of the specimen, some of the filter weights had to be applied to zero values of the signal. The phase unwrapping was performed by a counter that kept track of the rotation of the light vector¹³ and added jumps of phase π to close the gap between fringe ends. Conceptually, the whole process is not too different from the program that we use today except for great improvements in the hardware and software. In 1974,¹⁴ an expanded version of the same material was presented with additional techniques of smoothing of the final data.

Pattern Differentiation

In the spring meeting of SEM in 1982, an important step in the numerical processing of fringe data was introduced. One of the nagging problems for the techniques that measure displacements was the computation of strains, which is the ultimate objective of many of the stress analysis problems. Many schemes for the solution of this problem have been proposed. Different global and local numerical differentiation procedures have been implemented. All these techniques use polynomials either locally or globally. The selection of a polynomial biases the results because a certain functional form is assumed. An unbiased way to obtain derivatives is to use band-pass derivative filters in the frequency space. Derivatives can be obtained from fringe patterns without performing phase retrieval and unwrapping; time is saved and sources of error are eliminated. If we take the FT of I_q and I_p that appear in eq (7) and apply the rule of differentiation in the frequency plane where ξ and η are the frequency coordinates

that correspond to x and y , we have

$$F_{\xi_s} = -i\xi FT[I_p(x)] \quad (8)$$

and

$$F_{\xi_c} = -i\xi FT[I_q(x)], \quad (9)$$

where the subscript ξ indicates the derivative with respect to ξ , the subscript s indicates the sinusoidal component and the subscript c indicates the cosinusoidal component. Taking the inverse transforms, squaring, and adding the square root, we have

$$\frac{\partial \Psi_x(x)}{\partial x} = \frac{1}{I_o} \sqrt{\left(\frac{\partial I_p}{\partial x}\right)^2 + \left(\frac{\partial I_q}{\partial x}\right)^2}. \quad (10)$$

The same process can be applied to the other derivatives. The process of differentiation was applied to a holographic moiré pattern.

Integrated Recording and Processing System

In the 1980s, very important advances took place in the area of hardware in order to process images with a considerable reduction in the cost of the hardware. Taking advantage of these advances, an integrated system to record and process fringes was introduced in the spring meeting of SEM in 1985. Figure 6 shows the schematic representation of the system. Holographic moiré patterns were recorded and developed *in situ*. At this time, no PCs were available with the capability of handling image-processing hardware. A special computer was assembled with a bus with the speed required to communicate the components of the image processor. The computer was not fast enough to perform two-dimensional FTs in reasonable times; for this reason, data processing was carried out line by line. Several interesting problems were handled by this system. A study was carried out to determine the causes of failure of blades on a 6-inch turbine wheel of the space shuttle that was used in the landing system.¹⁶ An investigation was performed to measure the damage of marble and sandstone subjected to weathering and acid rain.¹⁷ Another interesting investigation was carried out for dynamic detection of standing ultrasound waves.¹⁸

Phase Retrieval and Simultaneous Noise Reduction

In 1986 at the spring meeting of SEM,¹⁸ a technique was introduced that can be applied to a carrier or, if the carrier cannot be detected, to carrier fringes.¹⁹ The technique is geared to process very low frequency modulation fringes; this means that the displacements within a fringe are very small. Equation (6) of the carrier fringes contains a noise term that, for very low values of the modulation function $\psi(x)$, may be of the same order of magnitude than the noise. The idea then is to use the matched filtered concept. Cross-correlating the signal with a sinusoid of the same frequency is equivalent to using a matched filter,

$$C_c(x) = \int_{-\pi}^{+\pi} \cos[\omega_c x + \Psi(x)] \cos[\omega_c(x+s) + \alpha] ds, \quad (11)$$

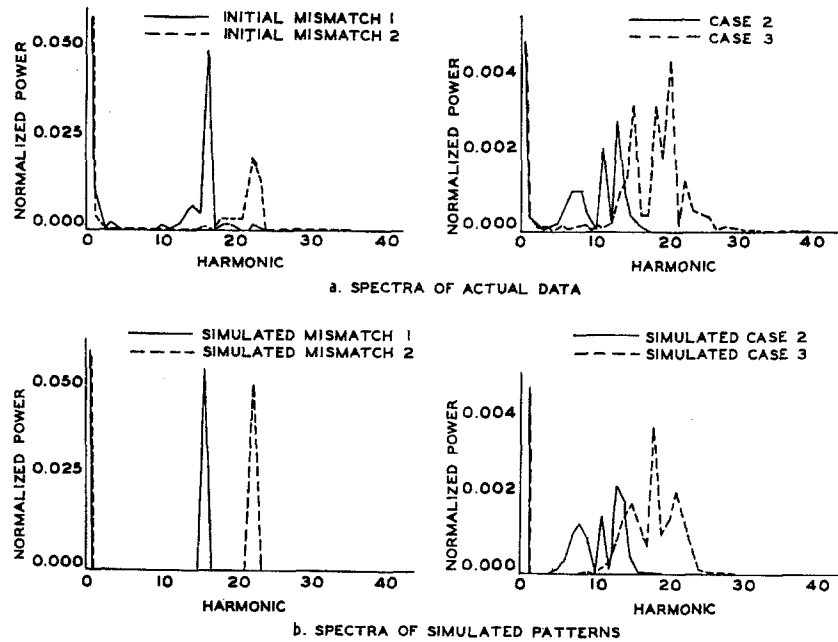


Fig. 5—FFTs of the patterns that provided the displacements and strain distributions given in Fig. 4 (1968)

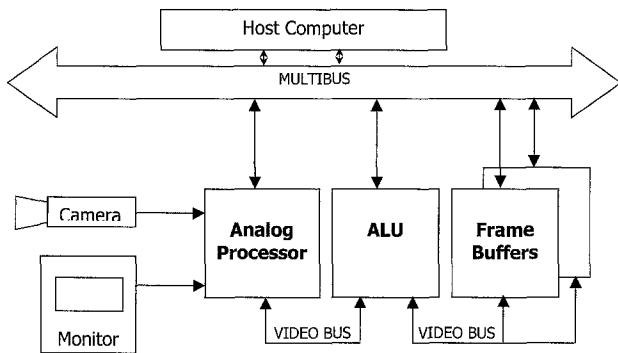


Fig. 6—Basic optical and electronic components of the system to record and process patterns (1985)

where $C_c(x)$ is the cross-correlation of the cosine term of the signal with a signal of the same frequency and phase angle α ; when the phase of the two signals is the same, the cross-correlation shows a maximum. The phase of the signal used to generate the cross-correlation with the experimental signal is modified stepwise until a maximum of the cross-correlation is obtained; the operation is performed pointwise. This technique was utilized to measure standing ultrasonic waves that were observed on the surface of a plate containing a hole.¹⁸ Figure 7 shows the specimen and the amplitude of vibration of the standing waves. Displacements of the order of 1 nm were accurately recorded. The fringe spacing corresponding to normal illumination and normal viewing is half of the wavelength of light, 314 nm (helium-neon laser). This implies a measurement of a fractional pitch of 1/314. Figure 8 shows the setup used to perform the measurements.

In 1989, at the ASME Symposium on Micromechanics, a new approach to phase determination was presented.²⁰ A

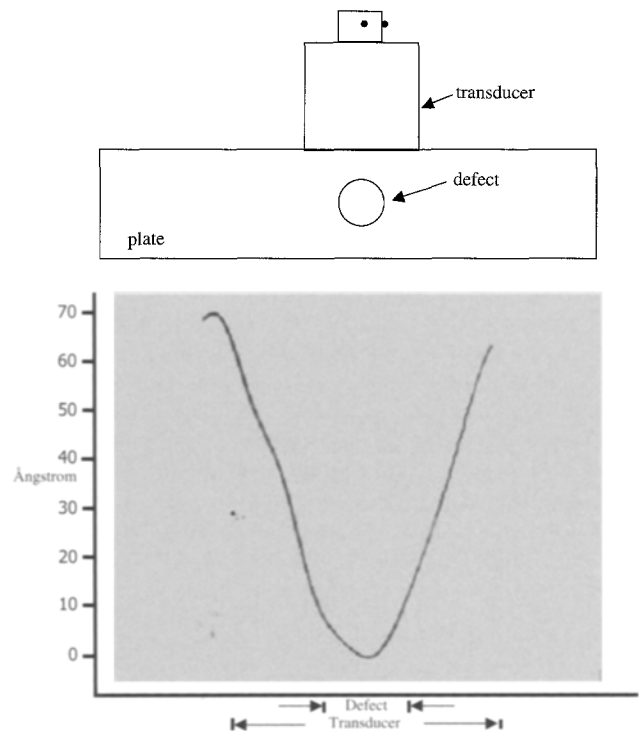


Fig. 7—Amplitude of vibration of ultrasonic standing waves (1 MHz) on the surface of a plate with a subsurface hole and excited by a transducer

PC-based imaging system was introduced with the capability of performing real-time operations in acquired images. The moiré pattern can be represented (eq (1))

$$I(x) = I_0 + I_1 \cos[\Psi(x) + \alpha]. \quad (12)$$

An initial phase α is added; for a given point, we can change α by optical means and the expression of the intensity at a point becomes a function of α . At a given point, we can take the FT of the signal using cosine and sine terms:

$$\text{Re } FT[I(x, \alpha)] = I_R = \int_0^{2\pi} I(x, \alpha) \cos \alpha \, d\alpha \quad (13)$$

$$\text{Im } FT[I(x, \alpha)] = I_{IM} = - \int_0^{\pi} I(x, \alpha) \sin \alpha \, d\alpha. \quad (14)$$

The intensity at a point of the fringe pattern can be represented by a complex function:

$$I(x) = M(x)e^{i\Psi(x)}. \quad (15)$$

The instantaneous phase can be computed:

$$\Psi(x) = \text{arctg} \frac{I_{IM}}{I_{Re}}. \quad (16)$$

The above scheme was implemented by optically shifting the phase of the illuminating beams. A program was written; in the discrete version, integrals were represented by summatories. It can be shown that the operation of multiplication by sine and cosine has the effect of filtering the signal. The specimen studied was a tensile specimen of a composite made with chopped fiber-glass fibers in an epoxy matrix. The region analyzed was the neighborhood of a fiber located perpendicular to the tensile direction. The observed region size was about $80 \times 80 \mu\text{m}^2$. The optical resolution of the microscope was about $1 \mu\text{m}$, and one pixel covered approximately one speckle. The observed patterns were holographic moiré patterns that we discuss later; the resulting equivalent pitch was $p = 0.337 \mu\text{m}$. An initial image was grabbed and stored in the memory. The specimen was loaded and the position of the image was restored using fiduciary marks. The phase steps were introduced using the technique described by Sciammarella and Lurowist.²⁸ Successive images were grabbed with increasing phase steps up to 2π . These patterns were used to run the computer program to obtain the phase at each pixel. The optical setup used in this study is shown in Fig. 9. The strains in a section perpendicular to a fiber are shown in Fig. 10. Minimum displacements measured were 2.5 nm or $p/135$.

Limits to the Continuous Optical Law

How far can the process of fractional pitch determination be pushed? At the outset of the introduction of the continuous optical law, it was postulated that the law was an instrument to increase the sensitivity of techniques that generate fringe patterns by measuring fractional fringe orders. Numerous applications indicated that this was indeed the case. However, the fundamental question of limits to this process remained unresolved. The first attempt to answer this question was presented at the spring meeting of SEM in 1990.²¹ The mathematical model of fringes as frequency-modulated signal was further expanded to show that the bandwidth of the carrier was a function of ϵ/p , the ratio of the strain and the pitch of the real or virtual carrier. It was also shown that, in order to decide the pitch of the grating to be used in a given case,

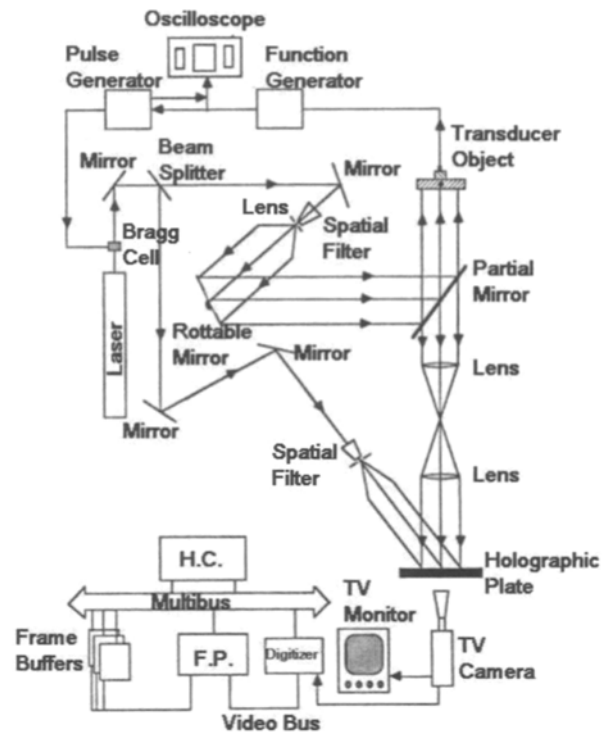


Fig. 8—Experimental setup to record and process ultrasonic standing waves of Fig.7; stroboscopic illumination

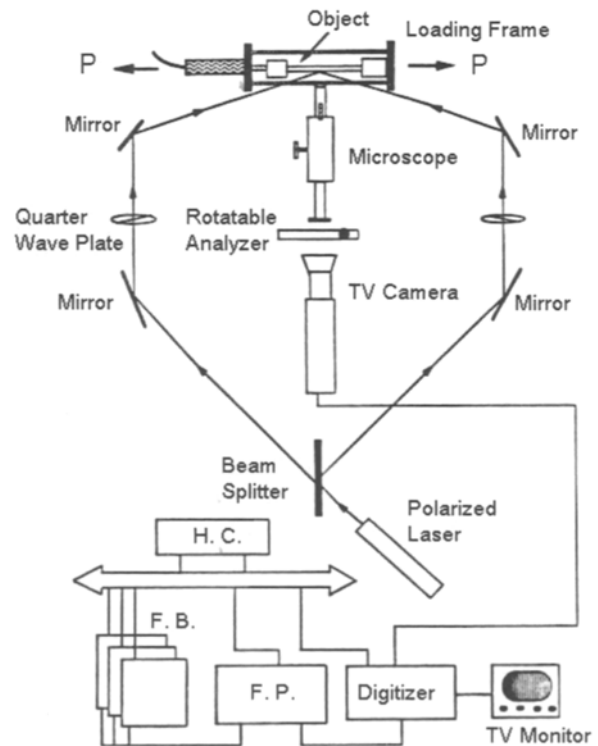
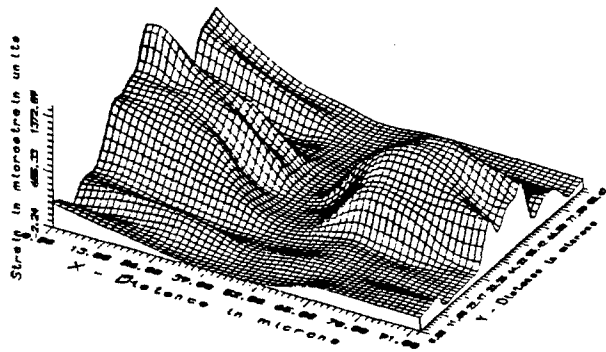


Fig. 9—Optical setup to record and process the displacement and strain fields in an epoxy short glass fiber reinforced composite



STRAIN CURVE

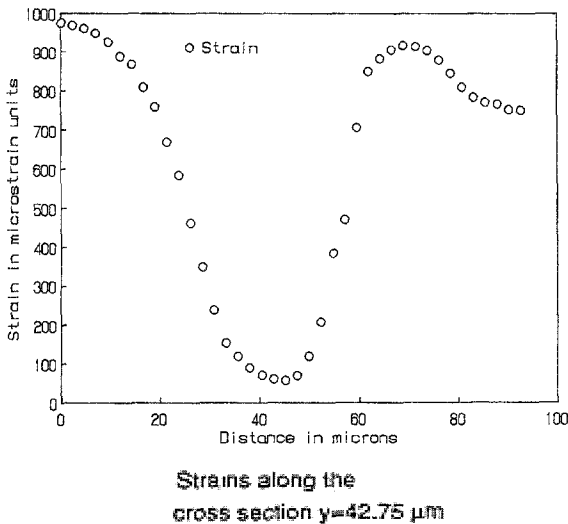


Fig. 10—Strain field obtained by the setup shown in Fig. 9 in the neighborhood of a short fiber perpendicular to the straining direction

we should use the Shannon–Whittaker theorem. According to this theorem, the spatial frequency of the carrier should be twice the highest spatial frequency that we want to detect. Once the deformed shape of the carrier or the moiré fringes are recorded, the Shannon–Whittaker theorem must be applied for the second time to determine the sampling rate of the recorded signal. There are two separate decisions to make but these decisions are connected to each other, since if we increase the frequency of the carrier we must also increase the sampling rate of the distorted carrier or the generated moiré fringes. Otherwise, the additional information generated by increasing the sampling of the displacement field will not be recovered.

To answer this question and the limits in the detection of fractional fringe orders, the following experiment was carried out. Utilizing the holographic moiré method, the displacements and strains along the diameter of a disk under diametrical compression were determined. Data were obtained for the same load with six different carrier pitches, from 1.22 to 0.365 μm . The final result indicated that the accuracy achieved in displacements and strains was the same regardless of the utilized carrier. These results have been analyzed in successive papers.^{22,23} These studies resulted in the formulation of the following principle similar to the Heisenberg indetermination principle of signal analysis:

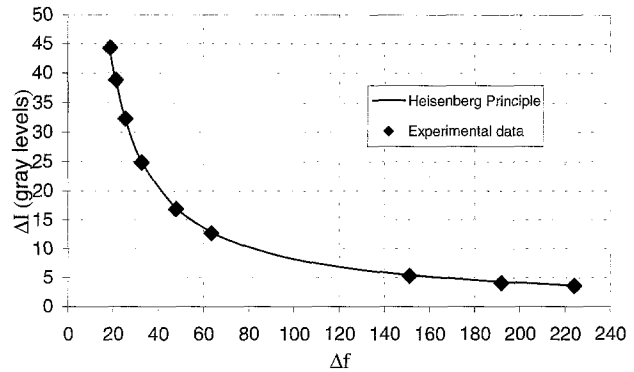


Fig. 11—Plot illustrating the application of the Heisenberg principle

$$\Delta I \Delta f = C. \quad (17)$$

This equation relates the accurately detected gray-level ΔI in a fringe pattern to the fractional order Δf that can be extracted from a frequency-modulated carrier or fringe. C is a constant that reflects the whole process to obtain displacement information. C is a function of the optical system, the device used to record the fringes, the numerical algorithms used to obtain displacement information. A very important consequence of eq (17) is that, for a given image size and a given recording camera, the frequency recovery once the Shannon–Whittaker theorem is satisfied does not depend on the frequency of the carrier. Figure 11 is a plot of eq (17) together with fractional orders recovered in experimental determinations that include moiré patterns, and holographic moiré patterns. Equation (17) is an important tool to design experiments. The above law and the experiments that support it dispel the common held belief that by just increasing the carrier frequencies it is possible to increase the accuracy of the obtained displacement and strains. A higher-frequency carrier may yield results that are less accurate than a properly selected lower-frequency carrier that has a better dynamic range.

Two-dimensional Fourier Methods for Fringe Pattern Analysis

In 1992,²⁴ the Fourier method of fringe pattern analysis that was initiated in 1966 came to a stage of maturity. The availability of faster PCs made it possible to generalize the required operations to two dimensions without getting into excessive computation times. The change from one to two dimensions is not as simple as may be construed. Between the continuous and discrete operations of filtering, there are factors of numerical approximation. While the line-by-line FTs have been quite successful in extracting noise, the two-dimensional operations have not reached the same level of efficiency. Generation of two-dimensional filters comparable to the sophisticated filters available in one dimension is not a simple task. This effect is particularly true in handling holographic moiré patterns. We adopted the following practical solution. The phase-stepping technique is used to initially extract phase information from a pattern. Four initial images are recorded with phase differences of 0, $\pi/2$, $3\pi/2$, π ; a similar

process is applied to the loaded patterns. The initial and final phases are computed by using the equation:

$$\Psi(x, y) = \arctg \frac{I^{270}(x, y) - I^{90}(x, y)}{I^0(x, y) - I^{180}(x, y)}. \quad (18)$$

Phase subtraction provides the phase of the loaded condition. This procedure can be applied to speckle patterns, and to moiré patterns when the carrier is recorded or an initial carrier is introduced. The computed phase is then encoded in fringes and the filter in the quadrature technique obtains the final filtered phase. This phase is used for the unwrapping procedure. The fact that filtered signals are used in the unwrapping considerably improves and simplifies final phase determination. Phase differentiation is performed on the filtered version of the phase.

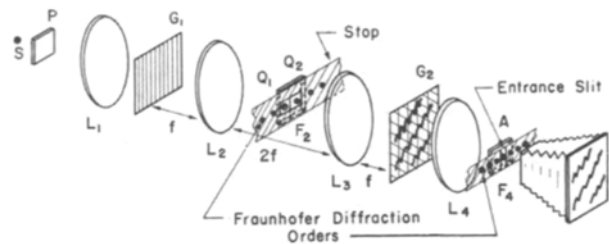
In our previous one-dimensional analysis, pattern extension beyond boundaries was performed by approximate methods. These methods did not work for two-dimensional problems. A fringe extension technique, based on work presented by Gerchenberg,²⁵ was implemented. Another question that has appeared many times in the literature of fringe analysis is whether the operations of data retrieval should be performed in coordinate space or in frequency space. Conceptually, there is no difference between these two modes of operation. However, there may be practical aspects that may influence the decision of using one of these two approaches. When we implement digital operations, we must consider the hardware, the software available, memory available, operational speeds and peripherals. Originally, when we introduced the Fourier method of fringe analysis, the software available to obtain fast Fourier transforms (FFTs) was at a stage that did not allow the necessary accuracy to perform filtering operations in the frequency space. With the advanced programs available today, there is a distinct advantage from the point of view of total required time to perform filtering operations in the frequency space.

Optical and Electro-optical Developments to Obtain Displacement, Contours and Strain Information

Optical Processing of Displacement Information

At the same time that the numerical procedures for numerical fringe pattern processing were being developed, efforts were being made in the area of purely optical procedures.

Another way to increase moiré fringe sensitivity was the use moiré interferometry. In the UK in the 1950s, Guild^{26,27} developed moiré interferometry for metrological purposes. Guild derived the fundamental equations of moiré interferometry and provided a number of examples of practical application of fringe multiplication. All these derivations were limited to metrological measurements of displacements using a pair of gratings. In 1966, at the Fifth National Congress of Applied Mechanics, we presented a full field interferometer to obtain a desired degree of multiplication.²⁸ Figure 12 shows the interferometer together with the device to implement phase stepping. Figure 13 shows a moiré interferometry pattern of a bar with a deep notch and the pattern multiplied three times. The same device was used for optical interpolation by phase stepping. The diffraction orders in the interferometer were circularly polarized in opposite directions and, by using an analyzer, the phase of the moiré fringes was modified making it possible to read fractional orders. Figure 14



S light source
P polarizer
L₁ collimating lens
L₂, L₃ telecentric lens system
G₁ model grid
Q₁, Q₂ quarter wave plates
G₂ master grating
L₄ imaging lens
A analyzer

Fig. 12—Moiré fringe interferometer for fringe interpolation and multiplication (1967)

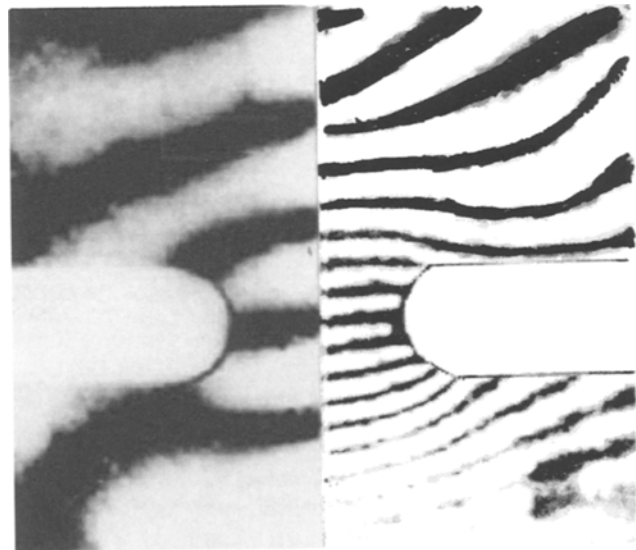


Fig. 13—Moiré interferometry pattern with a multiplication 3×. Tensile specimen with a notch (interferometer of Fig. 12)

shows the results of the determination of the strain at the root of the notch of the bar, as shown in Fig. 13.

The above interferometer was extensively used in Japan in the 1970s. The Japanese researchers realized that the first part of the interferometer was not required and that it could be replaced with a double beam illumination of a grating printed on a mirrored steel surface.²⁹ The replication technique and the double beam illumination were also applied by Walker and McKelvie.³⁰ The practical application of this technique to many engineering problems resulted from the developments introduced by Post and Barakat.³¹

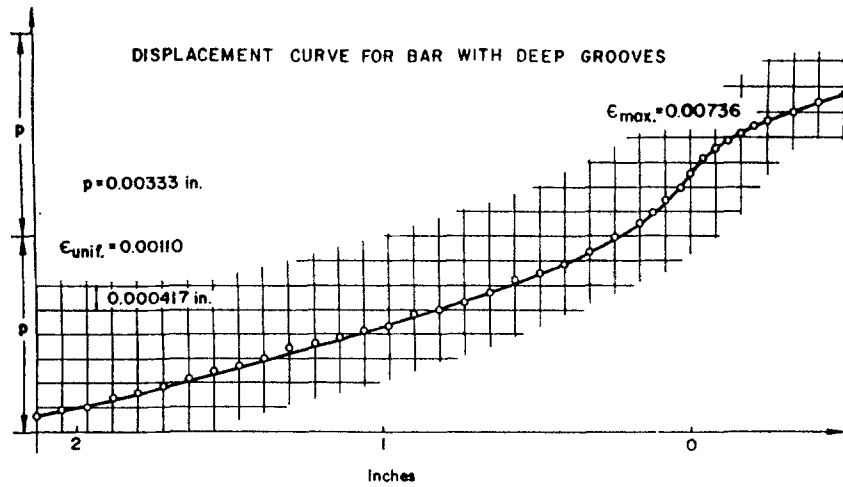


Fig. 14—Strain at root of the notched specimen shown in Fig. 13 by phase stepping obtained with the interferometer shown in Fig. 12

A simplified interferometric arrangement was presented at the spring meeting of SEM in 1968.³² Figure 15 shows the schematic representation of the optical system. The model grating is illuminated by coherent collimated light. Going through a lens system, the grating produces a Fraunhofer diffraction pattern; a stop allows only two orders to be recorded on a film. The interference of the two orders produces a grating of frequency $2np$ in the image plane of the lens system, where n indicates the selected order. No optical system is shown in Fig. 15 since this idea can be implemented by different lens arrangements; three lens arrangements have been analyzed by Sciammarella.³² The moiré pattern can be observed by putting back the developed film in the lens system, illuminating the film with collimated light and allowing one order to produce the image. Multiplications up to $20\times$ were obtained. If the loaded specimen grating is recorded twice with a shift between exposures, upon reconstruction a pattern of the derivatives is obtained, as shown in Fig. 16. At the fall meeting of SEM in 1969,³³ a technique of differentiation of moiré patterns was introduced, using replicas of the deformed grating. The replica was illuminated by collimated light. Self-replication of the grating in space was used to obtain a sheared image of the grating on a film located at some distance in front of the grating. After exposure and development, the film was placed in an optical filtering system and, at the image plane of the system, the pattern of the derivatives was recorded, after filtering the fringe order containing the moiré pattern (Fig. 17). This technique was further improved in 1974 by using the holographic recording of a selected diffraction order obtained from the replica of the deformed grating.³⁴ The angle of illumination was chosen so that the selected order of diffraction was perpendicular to the plane of the replica. By shifting between exposures the derivative was recorded. With a $25.4\ \mu\text{m}$ pitch, a derivative pattern corresponding to a pitch $p = 2.82\ \mu\text{m}$ was obtained. Since no lenses are used in this process there is no limitation on the diffraction order that can be used. Furthermore, another advantage is a property of holographic interferometry that was pointed out by Gabor: the ability of holographic interferometry to capture very low intensity wavefronts.

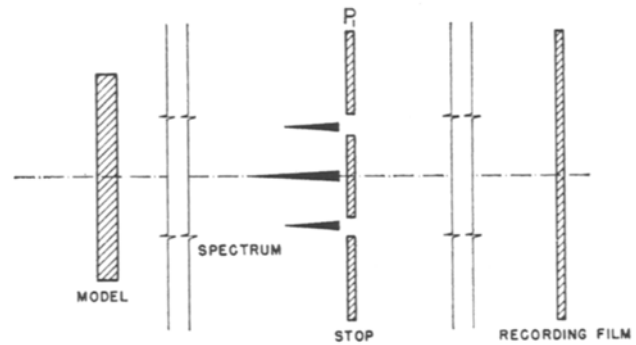


Fig. 15—Schematic representation of optical setups for fringe multiplication by wavefront reconstruction

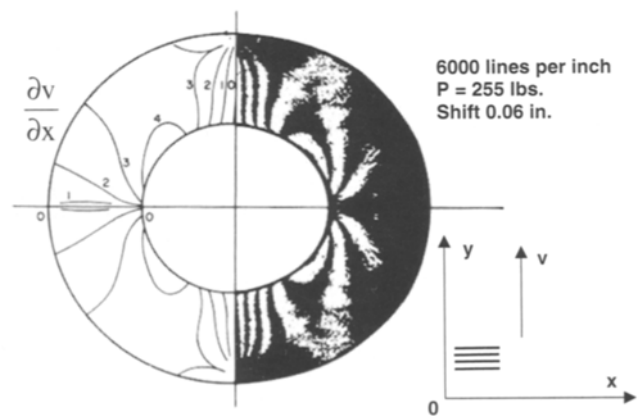


Fig. 16—Ring under diametrical compression pattern of $\frac{\partial v}{\partial x}$ obtained by replicating the loaded grating and shifting. Multiplication $20\times$. Original $p = 84.6\ \mu\text{m}$, multiplied pitch, $p = 4.23\ \mu\text{m}$

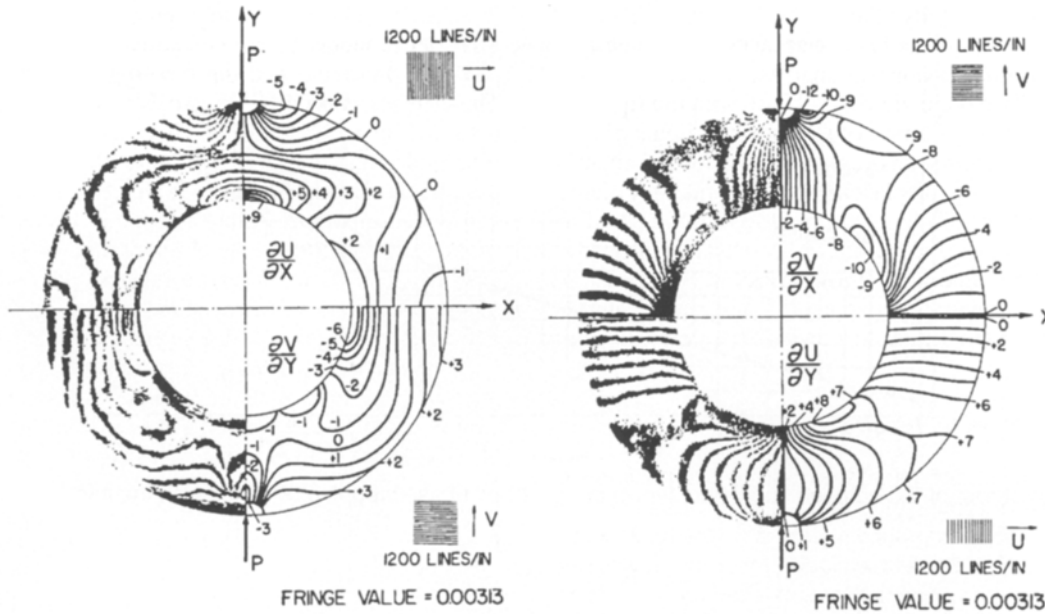


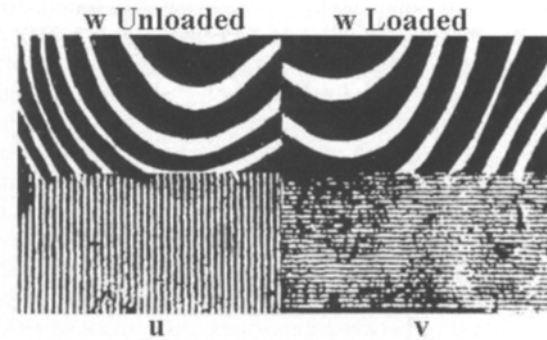
Fig. 17—Ring under diametrical compression. Derivatives of the displacements obtained by grating replication and shearing interferometry. The replicated gratings produced the shearing of the wavefronts

Moiré Holography

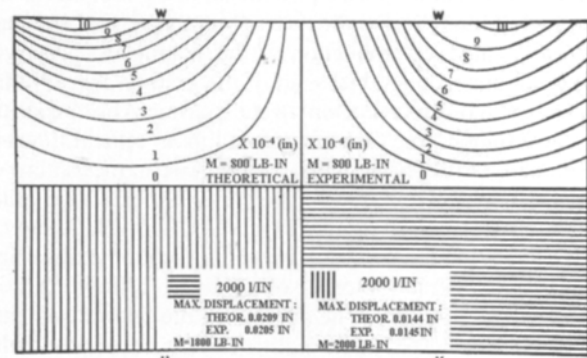
In some of the preceding examples, the recording of moiré patterns and their retrieval for further processing had a very close relationship with holographic procedures. This similarity led us to coin the term moiré holography. The recording of wavefronts on a light sensitive media, and the manipulation of diffraction orders to isolate given wavefronts that contained sought information, resulted in the extension of moiré to three dimensions beyond the cases of polar or spherical symmetry.³⁵ In-plane and out-of-plane displacements of plates were obtained. The displacements in the interior of a transparent body, a rectangular bar subjected to torsion, were obtained, as shown in Fig. 18. We can see in Fig. 18 the warping function (w displacements) and the u and v fields that correspond to a pure rotation of the cross-section. This technique has been used in Europe by several researchers to solve a number of engineering problems related to bending of plates with complex shapes.

Holography

Holographic interferometry in the earlier stages of development was connected to the moiré effect; in a number of publications, this relationship was pointed out. Likewise, moiré holography provides projected displacements. The main difficulty for practical applications of holography is the fact that, as pointed out in the 1971 ASME Symposium on Applications of Holography in Mechanics,³⁶ the projected displacements are given along the sensitivity vector, determined by the viewing and by the observation directions of the analyzed points. This property of holographic interferometry requires solving at least three equations with three unknowns for each analyzed point to obtain the components of the displacement vector in the same coordinate system. In order to obtain accurate results, it is necessary to have well-posed systems of equations, otherwise numerical errors become important.



(a)



(b)

Fig. 18—Moiré patterns of the displacements of a rectangular bar subjected to torsion. Two patterns are recorded for the displacement w to remove the beam-path changes produced by the lenses used in the optical bench: (a) patterns of u , v , and w (warping) displacements; (b) comparison of experimental and theoretical values

The first complete study of an elastic problem using holographic interferometry was presented in 1973.³⁷ A disk under diametrical compression was analyzed using holographic interferometry. Two main views combined with multiple secondary views and the solution of redundant systems of multiple equations with three unknowns, yielded the information necessary to obtain the displacements along the disk diameter (in plane and out-of plane components). In the Third International Congress of Experimental Mechanics in 1973,³⁸ the solution of a cylindrical shell clamped at both ends and subjected to a concentrated load using holographic interferometry was presented. Multiple views were utilized to obtain accurate results.

Holographic Moiré Technique

From the experience gained through the application of holographic interferometry, the following conclusion was arrived at. In order for holography to become a practical tool for the solution of experimental mechanics problems, it was necessary to simplify the process of information retrieval. From this observation came the idea of the holographic moiré technique. In moiré holography, from information projected onto a plane, three-dimensional information is recovered. The inverse process would be to project the three-dimensional information onto a plane. Ennos³⁹ observed that the displacement of a point could be projected onto a plane by viewing the point at equal angles from the normal. The counterpart would be to illuminate the surface with two symmetric beams. Still, this process generated two different holograms that needed to be analyzed. We concluded that moiré was the tool to directly retrieve the in-plane displacement.

Different approaches were tried to generate carrier fringes that could produce moiré patterns from the two holograms generated by double beam illumination. One of the alternatives was to rotate the body to produce carrier fringes; the other alternative was to rotate the holographic plate. A big problem for this solution was the fringe localization. A solution was presented at the spring meeting of SESA in 1975.⁴⁰ The solution was to rotate the holographic plate around a vertical axis parallel to the plate located in front of it. The distance of the axis of rotation to the plate was computed through an equation derived from the analysis of the fringe localization phenomena. Figure 19 illustrates the basis of the optical process to obtain moiré fringes from holographic fringes. Left and right beam illuminations of a disk under diametrical compression are given in (a) and (b), which when superimposed (c) do not produce clear moiré fringes. If carrier fringes are added (d), the superposition produces a moiré pattern (e); filtering this pattern we obtain (f) a moiré pattern. In 1975, this technique was extended to the observation of displacements in the interior of transparent bodies (Fig. 20). Through the phenomenon of scattering of the light by a transparent medium, it was possible to extend the application of the holographic moiré technique to the interior points of a transparent medium.⁴¹ In 1977, an extension of moiré holography to three-dimensional surfaces was presented. The displacements of a three-dimensional surface (Fig. 21) were projected onto a coordinate plane.⁴² Still, the technique posed the problem of having the recording plate on a device with an external axis of rotation. To rotate the plate around an axis located on the holographic plate lens, holography was introduced at the spring meeting of SESA in 1978.⁴³ The image of the ob-

ject is focused on the holographic plate and recorded with a reference beam. A mathematical model of lens holography was presented and the recording conditions analyzed. The displacements and derivatives of the displacements were obtained for a disk under diametrical compression and of a pipe under internal pressure. In 1979, at the IUTAM symposium on Optical Methods in Mechanics of Solids,⁴⁴ two additional important features were added to the holographic moiré technique: real-time observation by recording the initial hologram of the observed surface, developing the plate *in situ*, then loading the specimen and recording the moiré holographic fringes in real time using a TV camera (Fig. 22).

In place of generating the carrier fringes by rotating the plate, the reference beam rotation generated the carrier fringes. In this presentation, it was shown that all the possible operations with moiré, such as fringe multiplication and fringe differentiation by shifting, could also be performed in moiré holography. The observation of holographic moiré fringes in real time provides a very powerful tool for the observation of transient events. A detailed analysis of the problems of the holographic moiré technique in real time has been presented.⁴⁵ In 1982,⁴⁶ another important step in the holographic moiré technique was introduced. The relationship between holography and the holographic moiré technique was formalized through the transformations of the sensitivity vector. These transformations provide the basis of changes in the optical setup to obtain given components of the displacement vector. The connection between the holographic moiré technique and moiré was extended to contouring. A technique of contouring equivalent to shadow moiré was introduced. It was shown that by rotating the illumination beam it is possible to generate fringes that provide the contour lines of a surface with respect to a reference plane. Along the same line, a technique equivalent to reflection moiré was introduced. Equations were derived for the equivalent of reflection moiré. In the case of a reflective surface, if the illumination beam is rotated, fringes of equal slope are generated. Further work on different aspects of the holographic moiré contouring can be found in Sciammarella⁴⁷ where additional references on properties of holographic moiré contouring are given.

Three-dimensional Strain Analysis through Moiré Holography

With the introduction of the holographic moiré technique, the moiré method was extended from two-dimensional surfaces to general three-dimensional surfaces in a very practical way. Previous attempts were limited to cylindrical surfaces or required elaborate setups.⁴⁸ In holographic moiré, the components of the displacement vector are projected onto a single frame of reference. Displacements projected on a universal frame of reference cannot be used directly to compute strains on the surface under analysis. Strains have meaning only when a local frame of reference is used. To move from the universal to the local frame of reference, it is necessary to have a description of the geometry of the surface under analysis. The technique presented by Sciammarella⁴⁶ makes it possible to use the same optical setup to obtain displacements and contours. At the 1988 IMEKO meeting,⁴⁹ the necessary derivations were introduced and an example application was given to obtain from the universal to the local system. Figure 23 shows the moiré patterns corresponding to a cylinder under internal pressure. Figure 23 shows the direction

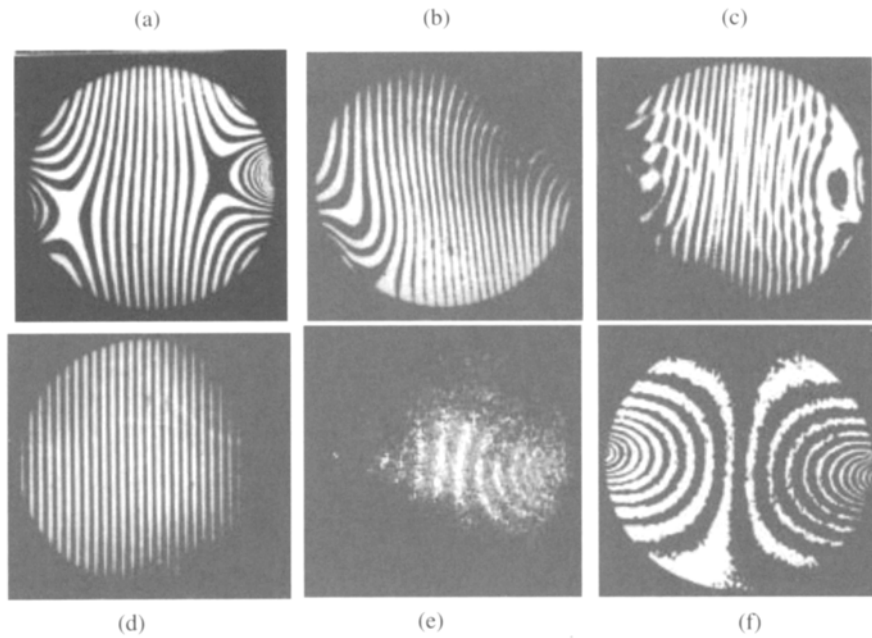


Fig. 19—Basic process for the formation of holographic moiré patterns

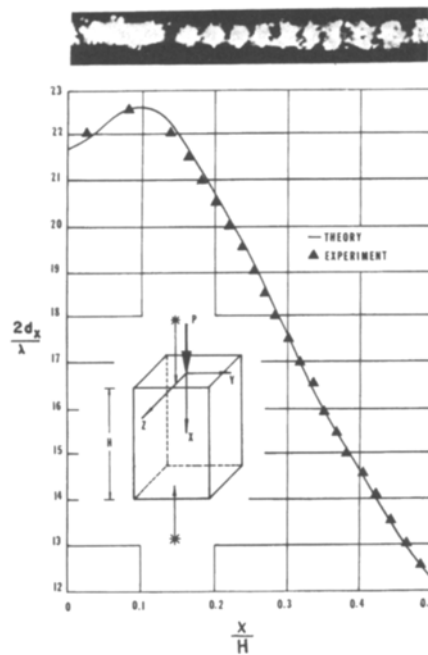
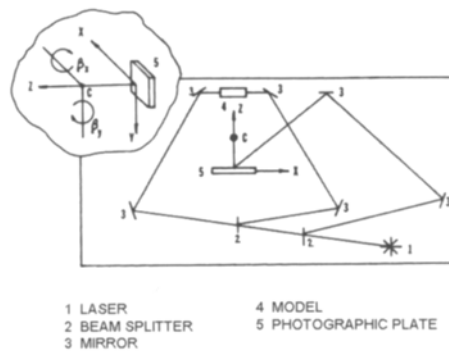


Fig. 20—Holographic moiré pattern of the vertical displacements in a semi-infinite plane obtained with double-beam illumination in a transparent medium. Theoretical values correspond to a semi-infinite plane with a concentrated load

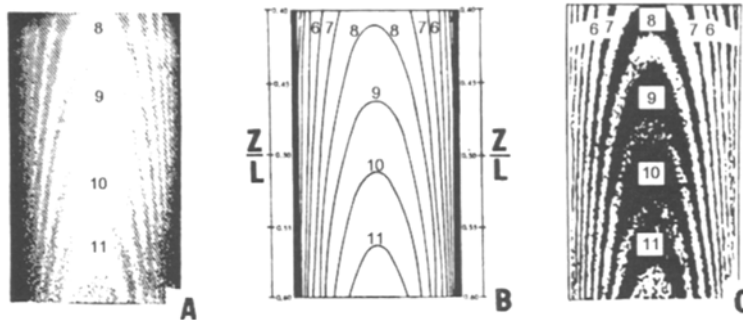


Fig. 21—Horizontal displacements of a circular bar subjected to torsion obtained by holographic moiré: (a) unfiltered holographic moiré; (b) theoretical loci of the displacements; (c) filtered holographic moiré

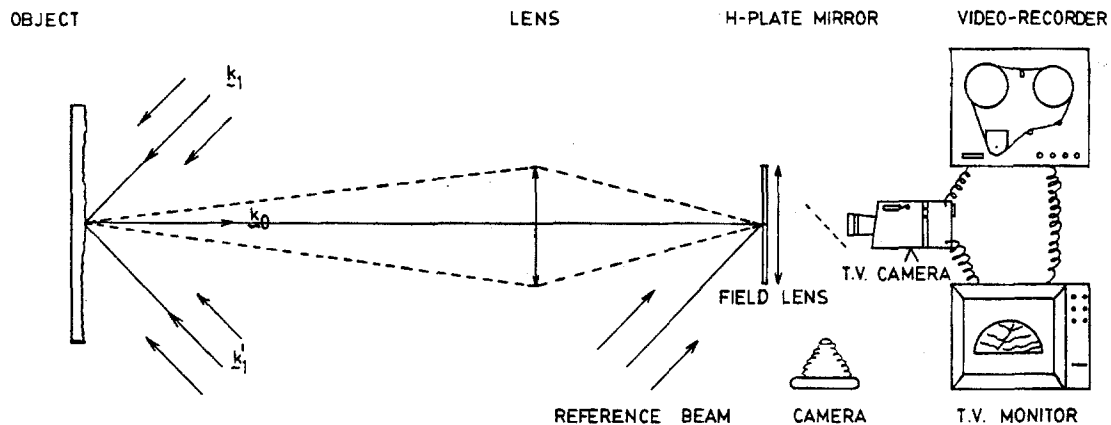


Fig. 22—Setup to record holographic moiré patterns in real time (1979)

of illumination of the recorded holographic moiré patterns. In the x_2 -direction, the left and right beams were separately recorded. From the two recordings by pattern multiplication and filtering, the displacements in the x_2 - and x_3 -directions were obtained. From these displacements, the moiré patterns shown in Fig. 23 were generated. Figure 24 shows the hoop strains obtained from the differentiation of the moiré patterns and transformation from the universal to the local frame of reference. In all the developments described above, the initial use of recording films was replaced later by the recording of patterns on light sensitive plastics. Finally, the use of electronic recording of the generated holographic patterns became an integral part of the utilized procedures.

Electronic Moiré Holography (Electronic Speckle Interferometry)

Speckle pattern interferometry is based on the same basic premises as holographic interferometry. Under the assumptions of small deformations and small rotations, a speckle pattern on a surface can be considered a point property of the surface. The speckle will experience the same changes that the surface experiences. A speckle pattern can be considered a random carrier of information. In the random signal, a deterministic signal is encoded, the displacement function of the surface. The three-dimensional displacement information is reduced to two-dimensional distributions of intensities by

the interactions of two wavefronts: the object wavefront and the reference wavefront. The loaded state speckle pattern is considered almost identical to the unloaded one, except for the fact that it contains a deterministic signal, a phase modulation of the carrier. To extract the deterministic component of the phase, it is necessary to superimpose the initial and the loaded states since our reference state is a random signal. If we do not have the initial random phase distribution, we cannot recover the modulation function.

The same equation, which in holographic interferometry relates the sensitivity vector to the change of optical path, is valid in speckle interferometry. Furthermore, the process of speckle recording is the same as the process used in lens holography. In lens holography, the recording is local.⁴³ The same local recording takes place in speckle interferometry. To this point, all the basic procedures of holography and speckle interferometry are identical. The difference comes in the process of extracting the deterministic signal from the random signal. In holography, optical reconstruction provides the correlation fringe patterns displaying the projected displacements. In speckle interferometry, there are many alternative ways of extracting the displacement information. In the original work of speckle interferometry, several procedures to obtain fringe patterns were proposed. The most commonly used is the subtraction of the unloaded specimen recording from the loaded specimen recording. Originally, this was done by

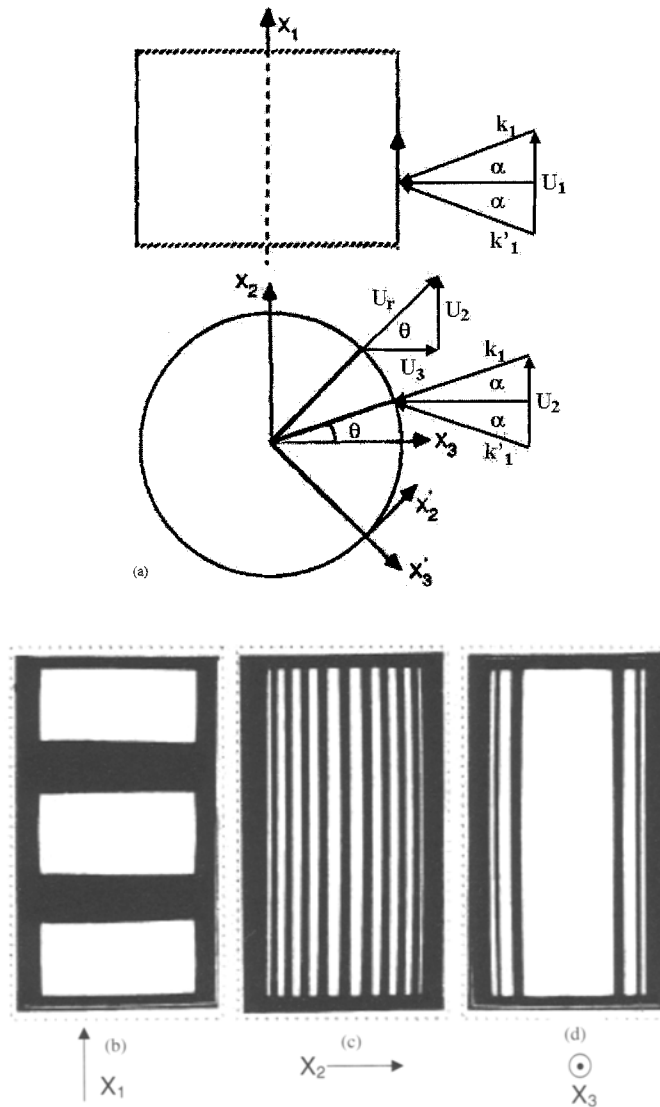


Fig. 23—Moiré patterns of a cylinder under internal pressure: (a) coordinates and directions of illumination; (b) moiré pattern, x_1 -direction; (c) moiré pattern, x_2 -direction; (d) moiré pattern, x_3 -direction. Pipe dimensions: O.D. = 48.72 mm, I.D. = 40.42 mm, thickness $t = 4.15$ mm, pressure 183.4 KN/m², $E = 275.8$ KN/m², $\nu = 0.35$, sensitivity $p = 10.54 \times 10^{-4}$ mm

superimposing a negative film with a positive film. A very important development in the technology of speckle interferometry was the use of a TV camera sensor to record the speckle patterns. With electronic recording, the subtraction of speckle patterns could be done within the framing time of the utilized camera. The basic procedures for the electronic recording of speckle patterns were developed almost simultaneously by Macovski, Ramsey, and Schaefer⁵⁰ in the USA, Schwomma⁵¹ in Austria, and Butters and Leedertz⁵² in the UK. We came to the realization that the process of generating carrier fringes required in holographic moiré interferometry was not needed in the recording of speckle patterns produced by double-beam illumination. The two beams acted as reference beams of each other. Reflecting on the close connection between holography and speckle interferometry, we started to use the nomenclature TV holography or electronic holography instead of the more usual nomenclature electronic speckle interferometry (ESPI).

In 1985 (Fig. 6), a system was presented to record patterns directly onto light sensitive media (CCD camera) and simultaneously to process data. The system was designed along the same lines of the system introduced earlier in the 1980s with the only addition that, in place of using a separate recording medium to collect the basic signals required to generate correlation fringe patterns, the CCD sensor was used to record these signals. In, 1993,⁵³ a portable electro-optical interferometer was introduced. The portable interferometer included the following innovations. Collimated light was used in all the previously described applications. In the in-plane sensitivity interferometer described by Sciammarella, Bhat, and Bayeux,⁵³ a point-source illumination was used. By properly selecting the recording geometry, the error introduced by replacing the collimated illumination by a point source is made negligible. The interferometer has the following additional properties. An active feedback control system compensates for the background vibrations and, at the same time, this

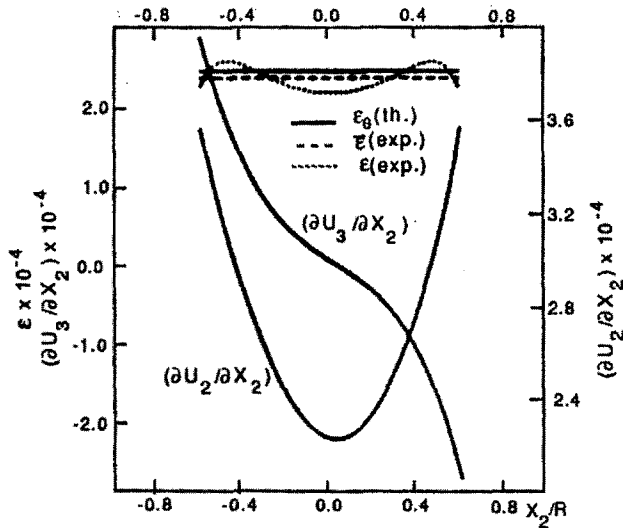


Fig. 24—Hoop strains obtained from the patterns shown in Fig. 23 through differentiation and coordinate transformation

system can be used to apply the phase stepping technique. The interferometer also has a rigid-body compensation mechanism; the camera and the illumination sources are rigidly attached. By providing the camera light-source system with three degrees of freedom, the rigid-body motion caused by loading the specimen can be eliminated. The above-described system was built with the following three main features of the system: (a) point illumination; (b) phase compensation; (c) rigid-body correction. The strain field of an aluminum disk under diametrical compression was determined. The angle of illumination was 17.25° . The phase stepping technique was used. The disk experienced a vertical motion of $75 \mu\text{m}$ and a rigid-body rotation. Both these motions were compensated. Very good agreement between theory and experiment were found.

At the 1998 Symposium of IUTAM,⁵⁴ two important innovations in the detection process of displacements were introduced. All the methods used in speckle interferometry are based on the separate recording of the components of displacements in two orthogonal directions. In this application, both components of displacement are recorded in one single frame. From this single frame, the two components are separated by numerical filtering in the frequency space. The second innovation is the process of removal of rigid-body motions, using a different approach to that of the previously described computer-controlled system. Fiduciary marks are utilized to make an approximate correction of the rigid-body motions. A final correction is made by using the fringes that the rigid-body motion produces in the FT space. The described methodology is applied to the analysis of microscopic fields of displacements and strains of a particulate composite with a viscoelastic matrix

The Holo-Moiré Strain Analyzer

All the experience gained, along with all the different developments that have been described, and the applications of these developments have culminated in the creation of a device called the Holo-Moiré Strain Analyzer (HMSA). The HMSA has a US patent 5,671,042 as of September 1997. Figure 25 shows one version of the instrument. The HMSA has a

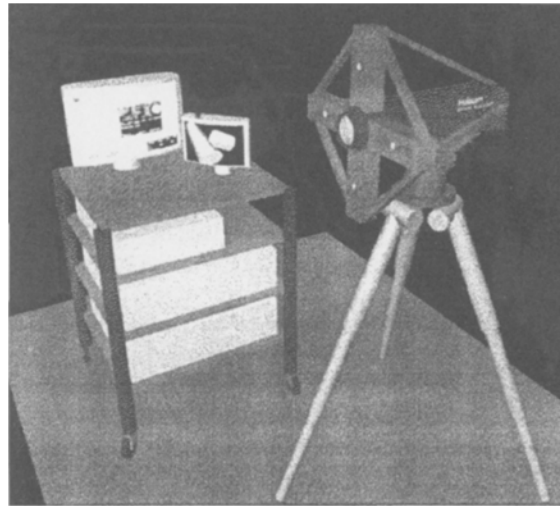


Fig. 25—Portable Holo-Moiré interferometer (1992)

fringe stabilization unit to eliminate the environmental vibration as described by Sciammarella, Bhat, and Bayeux.⁵³ The system also has the same system to correct rigid-body motions described by Sciammarella, Bhat, and Bayeux.⁵³ The dedicated hardware and software process the optical information in quasi real time. It has been in use both as a research tool and to solve commercial issues for the past 6 years.

Applications

Introduction

The techniques described above have a broad application in the development of technology (research and development) and in industry. They provide a powerful tool to investigate the performance of a product in service. For example, causes of failure of a product in service can be determined. They can also provide a tool to investigate the required remedy for observed failures. In recent years, there has been an explosive growth in the field of optical techniques. The growth has resulted from the increasing capabilities of optical techniques combined with computers. The synergy produced by the combination of advances in signal-processing methodology, the development of powerful algorithms and the use of faster computers with increasing memory capabilities has led to a new era in the use of optical techniques. These techniques are currently capable of solving many problems with a speed and accuracy that can match purely numerical techniques, while avoiding the pitfalls resulting from models that simulate the actual behavior of real structural components.

The techniques that we have developed have been applied to many different technical and engineering problems. Owing to a lack of space, it is not possible to enumerate all the cases that we have tackled. In what follows, we present a summary of problems to which we have contributed.

Hybrid Methods

Numerical integration of constitutive equations has been used to obtain stresses utilizing displacement fields measured using moiré fringe patterns in plasticity and viscoelasticity. The viscoelastic application was the study of a propellant

grain subjected to a sudden internal pressure. High-speed photography was used to record the moiré patterns giving the strain history of the propellant grain.

Composites

FIBER-REINFORCED COMPOSITES

Low-speed and high-speed moiré was utilized to study the fracture of single lamina covering the range of loading rates from 1.66 microstrain per ms, to 1.66×10^5 microstrain per ms. The moiré fringes were formed by the model grating and the master grating set in front of the tested specimen. A green laser was used to illuminate the specimens. In this study, interfacial stresses between the fibers and the matrix were also obtained from moiré data. The effect of matrix cracks on the fiber loads was also analyzed. In the case of short fiber composites, interfacial strains were microscopically determined using holographic moiré.

PARTICULATE COMPOSITES

As part of a comprehensive study of the behavior of aluminum matrix silicon carbide reinforced composite, interfacial strains in the microscopic range were studied using computer-aided moiré. The observed region was $100 \times 80 \mu\text{m}^2$ and the spatial resolution was 200 nm (Fig. 26). The experimental study was complemented with a finite-element study of a unit cell model of the composite.

The damage of propellant grains subjected to tensile loads and to cyclic loadings was studied using microscopy and holographic moiré. The damage analysis was performed by the statistical analysis of sampled regions. The statistical analysis was confirmed by an analysis of the changes of the propellant compliance determined using holographic moiré. A numerical analysis with finite elements and a unit cell model extracted from the experimental data provides an understanding of the development of damage by decohesion of the interfaces.

Ceramics

A program was carried out devoted to the non-destructive evaluation of defects of ceramics using holographic moiré. Methods to visualize and evaluate cracks down to the range of $200 \mu\text{m}$ were developed. Some of the experimental studies were validated by using finite-element simulations of the particular problem under consideration. The problem of evaluation of joints in ceramic components was also investigated. The integrity of ceramic fuel cells was investigated using holographic moiré.

Fracture Problems

The crack-tip region of a compact tension specimen was analyzed using computer-aided moiré. For analysis, a $12.5 \mu\text{m}$ grating was printed on a compact tension aluminum specimen, in which a crack was grown by fatigue loading. The crack propagation in notched rings simulating the cladding of a nuclear reactor component subjected to high temperature and internal pressure was investigated using moiré. A 12-lines/mm grating was etched on the surface of the specimens. The grating was photographically recorded as the specimen was loaded and heated. Using the photographic replica, moiré patterns with fringe multiplication were obtained in an

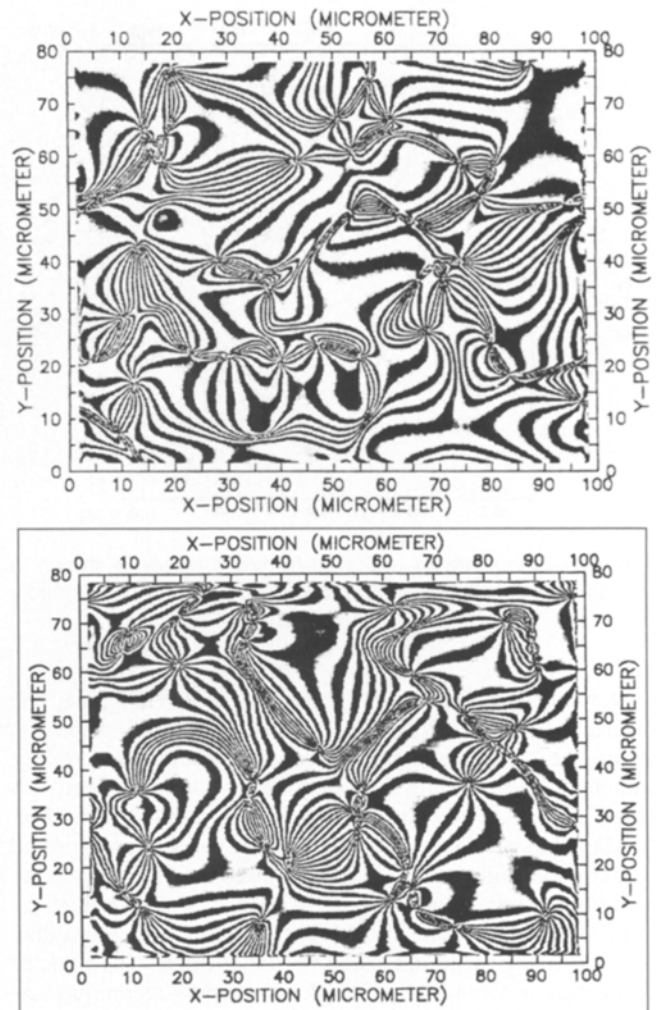


Fig. 26—Super-resolution moiré images of the u and v displacement fields on a region of tensile specimen made out of aluminum matrix reinforced with silicon carbide particles. Equivalent grating of pitch 55 nm

optical bench. A crack-opening displacement analysis and a J-integral analysis of the results were performed.

Residual Stresses

Residual strains and stresses in piping subjected to temperature gradients were investigated using moiré. The piping was simulated by a metallic ring heated by induction heating. Deformations were recorded as the specimen was heated by forming moiré fringes with a master grating located in the image plane of the camera. The master grating was in contact with a recording film. After cooling, the final residual strains were determined. By removing successive layers of the ring, the residual elastic stresses were determined. From the residual elastic stresses, the elastic residual strains were computed. By subtracting the elastic residual strains from the final residual the plastic residual strains were evaluated. Moiré patterns were recorded at each step of material removal.

Residual plastic strains were determined in the area of contact of a simulated wheel and rail. A grating was etched on the surface of the rail. Normal and tangential loads were applied. The deformed grating was copied by using a contact

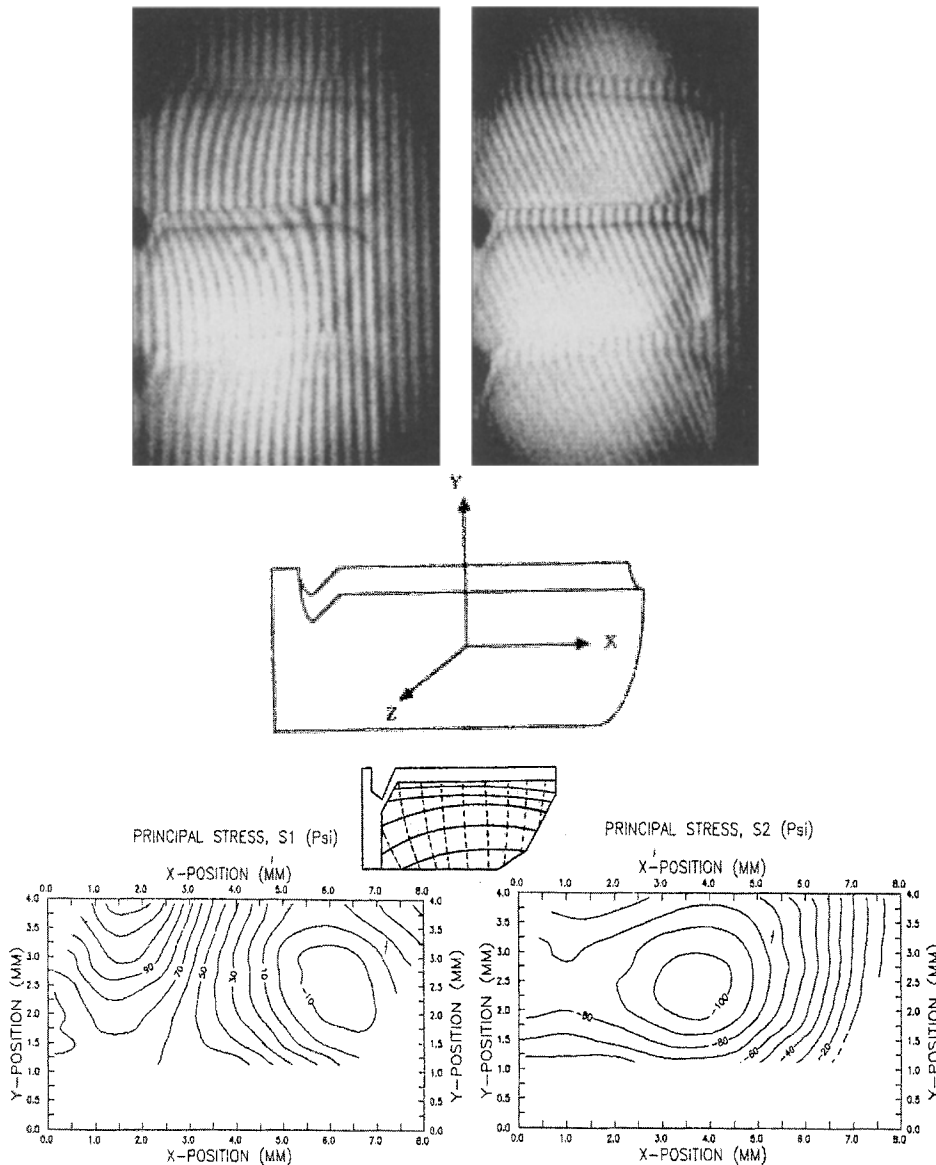


Fig. 27—Principal stresses and direction of a turbine blade of the SRB APU space shuttle turbine wheel obtained with the optical setup shown in Fig. 8

replicating technique. The moiré fringes were produced in an optical bench. Comparisons were made of the obtained results and some of the existing contact theories.

Residual stresses in silicon wafers during the process of fabrication of electronic chips were determined by using reflection moiré. Residual stresses in the electronic chips after the chips were cut from the wafer were also determined. The residual stresses were evaluated by measuring the curvature radii and relating curvatures to bending stresses.

Residual stresses were measured on ceramic electronic chips with metallic inserts. Holographic moiré contouring was used to measure curvatures and holographic moiré was used to measure strains caused by temperature changes. Curvature changes were related to bending stresses.

High-temperature Strain Measurements

Techniques were developed to measure strains up to 1000°C using holographic moiré. Utilizing a disk under dia-

metrical compression, elastic moduli were evaluated at high temperatures for a high-strength nickel alloy, and an excellent agreement was obtained with the values provided by the manufacturer.

Dynamic Studies

Holographic moiré contouring and holographic moiré are utilized to analyze the vibration modes and the stresses caused by the vibration modes in turbine blades, and rotating machinery. The patterns are recorded in real time by using stroboscopic illumination. An interesting analysis was carried out on the SRB APU turbine wheel for the space shuttle.¹⁶ Figure 27 shows two patterns: one pattern corresponds to the contouring pattern, and the other pattern is the pattern of the stroboscopic vibration pattern. From the holographic moiré pattern, strains were determined and principal stresses were computed using the methodology for three-dimensional holographic moiré determination of strains.

Contouring of Surfaces

Projection moiré contouring was applied to biomedical studies of malformation in joints. Holographic moiré contouring was utilized to measure loss of mass of marble and sandstone samples due to weathering and acid rain. Samples were exposed in different regions of the US and brought back to the laboratory for measurements. The study lasted nine years. Good correlations were obtained with direct mass lost by weight measurement. High-precision projection moiré has been used to perform metrological measurements in gear teeth. The projection moiré method produces measurements of the same degree of accuracy as expensive mechanical tactile machines.

Future Developments

It is not an easy task to predict the future, but there are already some more advanced methods for signal analysis that are applied to fringe patterns. In the development of a sensor to measure pressures in a wind tunnel wall, we have used a neural network to recognize levels of change of a moiré pattern of a deflected membrane in real time (time of operation of a standard TV framing). Traditionally, the methods that we have described in this paper are assumed to be techniques that measure displacements. However, if we modify the process of fringe pattern analysis and from the frequency modulated signal we extract the frequency, we can go directly from fringes to strains without the use of shear interferometry. Figure 28 illustrates an application of the ridge theorem of signal analysis that provides frequencies directly in the coordinate space.⁵⁵ The theorem, together with better filtering that can be achieved using wavelets, may greatly improve the process of fringe processing.

We should expect to have dedicated hybrid optical and electronic systems to process fringe information in real time.

All the current methods can be applied to the external surfaces of opaque materials. Internal surfaces have been accessible only for transparent media either by introducing a grating inside the material or by using light scattering as shown in Sciammarella and Gilbert.⁴¹ Internal points of opaque materials are accessible only by neutron diffraction. It will be of great interest to obtain a field technique that could be applied to opaque media.

Acknowledgment

All the work presented in this paper would not have been possible without the devotion, dedication, capability and skills of a large number of students and post-doctoral fellows. The names of most of these are in the different publications contained in the text. To all of them go my most sincere thanks and recognition.

References

1. Dantu, P., "Utilization des Réseaux pour L'Etude des Déformations," *Rapport de Recherche No 57-6, Paris, France, Laboratoire Central de Ponts et Chaussées*, 26-46, (1957).
2. Durelli, A.J. and Parks, V.J., *Moiré Analysis of Strain*, Prentice-Hall, Englewood Cliffs, NJ (1970).
3. Sciammarella, C.A., "Theoretical and Experimental Study of Moiré Fringes," *Doctoral dissertation, Illinois Institute of Technology, Chicago, IL* (1960).
4. Tardy, H.L., "Méthode Pratique d'Examen et de Mesure de la Biréfringence des Verres d'Optique," *Revue d'Optique*, **8**, 59-69, (1929).
5. Vinkier, A. and Dechaene, R., "Use of the Moiré Effect to Measure

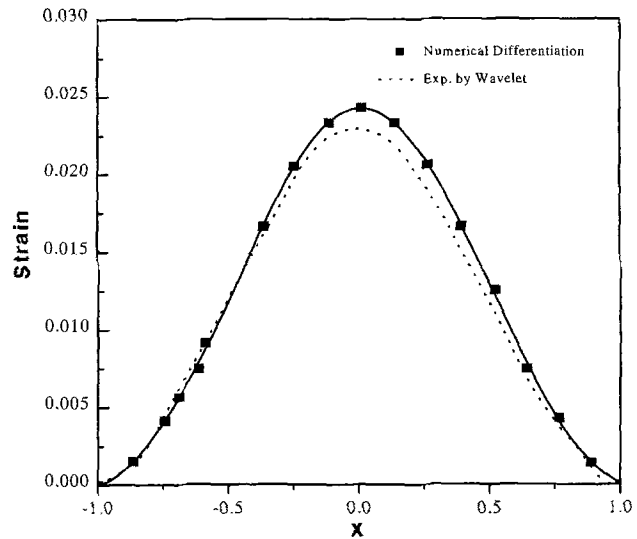


Fig. 28—Disk under diametrical compression; strains obtained directly from a moiré fringe pattern using the ridge theorem and wavelet transform. Data are the same as those used to obtain the results shown in Fig. 4

Plastic Strains," *Metals Engineering Conference 29 April-3 May 1959, Albany, NY, American Society of Mechanical Engineers, Paper no 59-Met7* (1959).

6. Sciammarella, C.A., "Basic Optical Law in the Interpretation of Moiré Patterns Applied to the Analysis of Strains I," *EXPERIMENTAL MECHANICS*, **5**, 154-160 (1965).

7. Ross, B.E., Sciammarella, C.A., and Sturgeon, D., "Basic Optical Law in the Interpretation of Moiré Patterns Applied to the Analysis of Strains II," *EXPERIMENTAL MECHANICS*, **5**, 161-166 (1965).

8. Sciammarella, C.A., "Technique of Fringe Interpolation in Moiré Patterns," *EXPERIMENTAL MECHANICS*, **7**(11), 19-30 (1967).

9. Sciammarella, C.A. and Sturgeon, D., "Substantial Improvement in the Processing of Moiré Data by Optical and Digital filtering," *Proc. 3rd Int. Congress of Experimental Stress Analysis, West Berlin*, 79-83 (1966).

10. Sciammarella, C.A. and Sturgeon, D., "Digital Techniques Applied to the Interpolation of Moiré Fringe Data," *EXPERIMENTAL MECHANICS*, **7**(11), 468-475 (1967).

11. Sciammarella, C.A. and Doddington, C.W., "Effect of Photographic-Film Nonlinearities in the Processing of Moiré Fringe Data," *EXPERIMENTAL MECHANICS*, **7**(9), 398-402 (1967).

12. Sciammarella, C.A., "A Numerical Technique of Data Retrieval from Moiré or Photoelasticity Patterns," *Pattern Recognition Studies, Proc. SPIE*, **18**, 92-101 (1969).

13. Doddington, C.W., "Study of Numerical Techniques Useful in Moiré Fringe Data Analysis," *M.S. Thesis, University of Florida at Gainesville* (1967).

14. Sciammarella, C.A. and Rowland, E., "Numerical and Analog Techniques to Retrieve and Process Fringe Information," *Proc. 5th Int. Conf. on Experimental Stress Analysis, Udine, Italy, G. Bartolozzi, ed.*, 1-43-1.52 (1974).

15. Sciammarella, C.A. and Narayanan, R., "The Determination of Components of the Strain Tensor in Holographic Interferometry," *EXPERIMENTAL MECHANICS*, **24**(4), 257-264 (1984).

16. Sciammarella, C.A. and Amadshahi, M.A., "Computer-aided Holographic-moiré to Determine the Strains in Arbitrary Surfaces Vibrating in the Resonant Mode," *Proc. 1989 SEM Spring Conference*, 579-587 (1989).

17. Sciammarella, C.A. and Amadshahi, M.A., "Holographic Interferometric Method for Assessment of Stone Surface Recession and Roughening Caused by Weathering and Acid Rain," *Proc. IMEKO Int. Conf. on State Static and Dynamic Parameters of Structures and Materials, Pilsen, Czechoslovakia, Vol. 2*, 486-494 (1987).

18. Sciammarella, C.A., Amadshahi, M.A., and Subbaramanian, B., "Holographic Measurement of Ultrasonic Vibration Amplitudes," *Proc. 1986 Spring Meeting SEM*, 706-710 (1986).

19. Sciammarella, C.A., Amadshahi, M.A., and Subbaramanan, B., "A Computer Base Method for the Analysis of Interferograms with Phase Changes Smaller than 2π ," *Proc. 1987 SEM Spring Conference on Experimental Mechanics*, 579–586 (1987).
20. Sciammarella, C.A., Bhat, G., Longinow, N., and Zhao, M., "High Accuracy Micromechanics Displacement Measurement Optical Technique," *ASME* **102**, 121–132 (1989).
21. Sciammarella, C.A., Bhat, G. and Albertazzi, A.A., "Analysis of the Sensitivity and Accuracy in the Measurement of Displacements by Means of Interferometric Fringes," *Holographic Interferometry and Speckle Metrology*, *Proc. SEM*, 310–320 (1990).
22. Sciammarella, C.A. and Sciammarella, F.M., "Heisenberg Principle Applied to Fringe Analysis," *Laser Interferometry X: Applications*, Gordon Brown, Werner P.O. Jupner, Ryszard Pryputmiewicz, eds., *Proc. SPIE* **4101**, 294–303 (2000).
23. Sciammarella, C.A. and Sciammarella, F.M., "Heisenberg Principle Applied to the Analysis of Speckle Interferometry Fringes," *Opt. Lasers Eng.*, in press (2002).
24. Sciammarella C.A. and Bhat, G., "Two-dimensional Fourier Transform Methods for Fringe Pattern Analysis," *Proc. VII Int. Congress in Experimental Mechanics*, 1530–1537 (1992).
25. Gerchenberg, G.W., "Super Resolution through Error Energy Reduction," *Opt. Acta*, **21**(9), 709–720 (1974).
26. Guild, J., *The Interference Systems of Crossed Diffraction Gratings, Theory of Moiré Fringes*, Clarendon Press, Oxford (1956).
27. Guild, J., *Diffraction Gratings as Measuring Scales, Practical Guide to the Metrological Use of Moiré Fringes*, Oxford University Press, Oxford (1960).
28. Sciammarella, C.A. and Lurowist, N., "Multiplication and Interpolation of Moiré Fringe Orders by Purely Optical Techniques," *J. Appl. Mech. E*, **34**(2), 425–430 (1967).
29. Otha, A., Kosuge, M., and Sasaki, F., "Measurement of Strain Distribution by the Moiré Fringe Multiplication Method at a Tip of Propagating Fatigue Crack," *Int. J. Fracture*, **13**(3), 289–300 (1977).
30. Walker, C.A. and McKelvie, J., "A Practical-multiplied Moiré System," *EXPERIMENTAL MECHANICS*, **10**(8), 316–320 (1978).
31. Post, D. and Baracat, W., "High Sensitivity Moiré Interferometry," *EXPERIMENTAL MECHANICS*, **21**(3), 100–104 (1981).
32. Sciammarella, C.A., "Moiré Fringe Multiplication by Means of Filtering and Wave Front Reconstruction Process," *EXPERIMENTAL MECHANICS*, **9**(4), 179–185 (1969).
33. Sciammarella, C.A. and Chang, T.Y., "Optical Differentiation of Displacement Patterns Using Shearing Interferometry by Wavefront Reconstruction," *EXPERIMENTAL MECHANICS*, **11**(3), 97–104 (1971).
34. Sciammarella, C.A., "Determination of Strains by Applying. Holographic Shearing Interferometry to Techniques That Provide Displacement Information," *Progress in Experimental Mechanics*, (Durelli Anniversary Volume), V.J. Parks, ed., *The Catholic University of America* (1975).
35. Sciammarella, C.A., Di Chirico, G., and Chang, T.Y., "Moiré Holographic Technique for Three-dimensional Analysis," *J. Appl. Mech. E*, **37**, 180–185 (1970).
36. Sciammarella, C.A., "Moiré Analysis of Displacements and Stress Fields," *Symposium on Applications of Holography in Mechanics*, W. Gottenberg, ed, *American Society of Mechanical Engineers*, NY, 51–88 (1971).
37. Sciammarella, C.A. and Gilbert, J.A., "Strain Analysis of a Disk Subjected to Diametrical Compression by Means of Holographic Interferometry," *Appl. Opt.*, **12**(8), 1951–1956 (1973).
38. Sciammarella, C.A. and Chang, T.Y., "Holographic Interferometry Applied to the Solution of a Shell Problem," *EXPERIMENTAL MECHANICS*, **14**(6), 217–234 (1974).
39. Ennos, A.E., "Measurement of In-plane Surface Strain by Holographic Interferometry," *J. Phys. E: Sci. Instrum.*, **1**(7) 731–734 (1968).
40. Sciammarella, C.A. and Gilbert, J.A., "A Holographic-moiré to Obtain Separate Patterns for Components of Displacement," *EXPERIMENTAL MECHANICS*, **16**(6), 215–220 (1976).
41. Sciammarella, C.A. and Gilbert, J.A., "Holographic Interferometry Applied to the Measurement of Displacements of the Interior Points of Transparent Bodies," *Appl. Opt.*, **15**(9), 2176–2182 (1976).
42. Gilbert, J.A., Sciammarella, C.A., and Chawla, S.K., "Extension to 3-D of a Holographic-moiré Technique to Separate Patterns Corresponding to Components of Displacement," *EXPERIMENTAL MECHANICS*, **18**(9), 321–327 (1978).
43. Sciammarella, C.A. and Chawla, S.K., "A Lens Holographic-moiré Technique to Obtain Components of Displacements and Derivatives," *EXPERIMENTAL MECHANICS*, **18**(10), 373–381 (1978).
44. Sciammarella, C.A., "Holographic-moiré," *Proc. 1979 IUTAM Symposium on Optical Methods in Mechanics of Solids*, A. Lagarde, ed., Sijhoff and Noordhoff, The Netherlands, 147–176 (1981).
45. Sciammarella, C.A., Rastogi, P., and Jacquot, P., "Holographic-Moiré in Real Time," *EXPERIMENTAL MECHANICS*, **22**(1), 52–63 (1982).
46. Sciammarella, C.A., "Holographic-moiré, an Optical Tool for the Determination of Displacements, Strains, Contours and Slopes of Surfaces," *Opt. Eng.*, **21**(3), 447–457 (1982).
47. Sciammarella, C.A., "Computer-assisted Holographic-moiré Contouring," *Opt. Eng.*, **39**(1), 99–105 (2000).
48. Wadsworth, N., Marchant, M., and Billing, B., "Real-time Observation of In-plane Displacements of Opaque Surfaces," *Opt. Laser Technol.*, **5**, 119–123 (1973).
49. Sciammarella, C.A. and Amadshahi, M.A., "A Computer Based Holographic Interferometry to Analyze 3-D Surfaces," *IMEKO XI, Proc. Int. Congress of IMEKO, Houston, TX, (Metrology)*, 167–175 (1988).
50. Makovski, A., Ramsey, S.D., and Schaefer, L.F., "Time-lapse Interferometry and Contouring Using Television System," *Appl. Opt.*, **10**(12), 2722–2727 (1971).
51. Schwomma, O, Austrian Patent No 298830 (1972).
52. Butters, J.N. and Leedertz, J.A., "Speckle Pattern and Holographic Techniques in Engineering Metrology," *Opt. Laser Technol.*, **3**, 26–31 (1971).
53. Sciammarella, C.A., Bhat, G., and Bayeux, P., "A Portable Electro-optical Interferometer," *Proc. Conf. on Advanced Technology in Experimental Mechanics*, The Japan Society of Mechanical Engineers, Tokyo, 155–160 (1993).
54. Sciammarella, C.A. and Sciammarella, F.M., "An Extension of Holographic-moiré to Micromechanics," *IUTAM Symposium on Advanced Optical Methods and Applications in Solid Mechanics*, 1998. A. Lagarde, ed., *Kluwer Academic Publishers, Dordrecht*, 451–466 (2000).
55. Sciammarella, C.A. and Kim, T.C., "Direct Determination of Strains from Fringe Patterns," *Proc. SEM 2002 Spring Meeting* (2002).